Theoretical aspects of C13 metabolic flux analysis with sole quantification of carbon dioxide labeling

Guangquan Shi

04/28/06

Omes?

- One June 26, 2000 President Clinton, with J. Craig Venter, left, and Francis Collins, announces completion of "the first survey of the entire human genome."

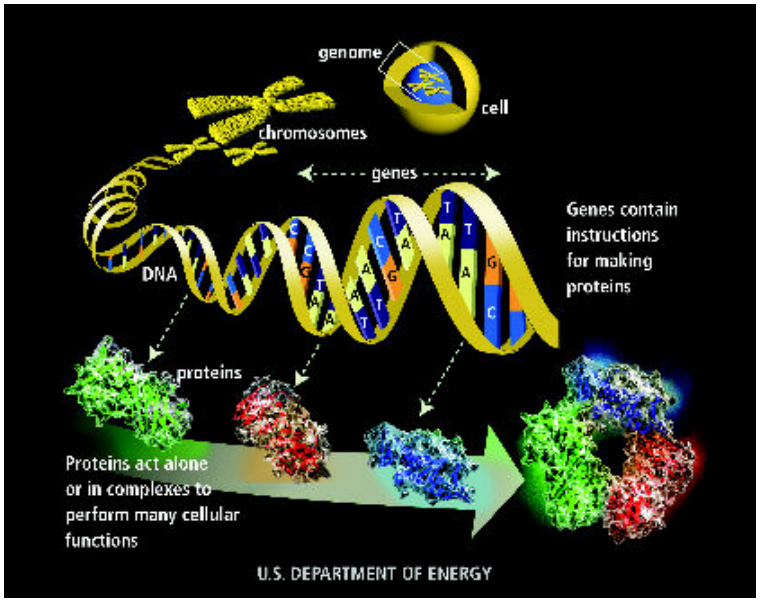

http://www.ornl.gov/TechResources/Human_Genome/home.html

Proteomics

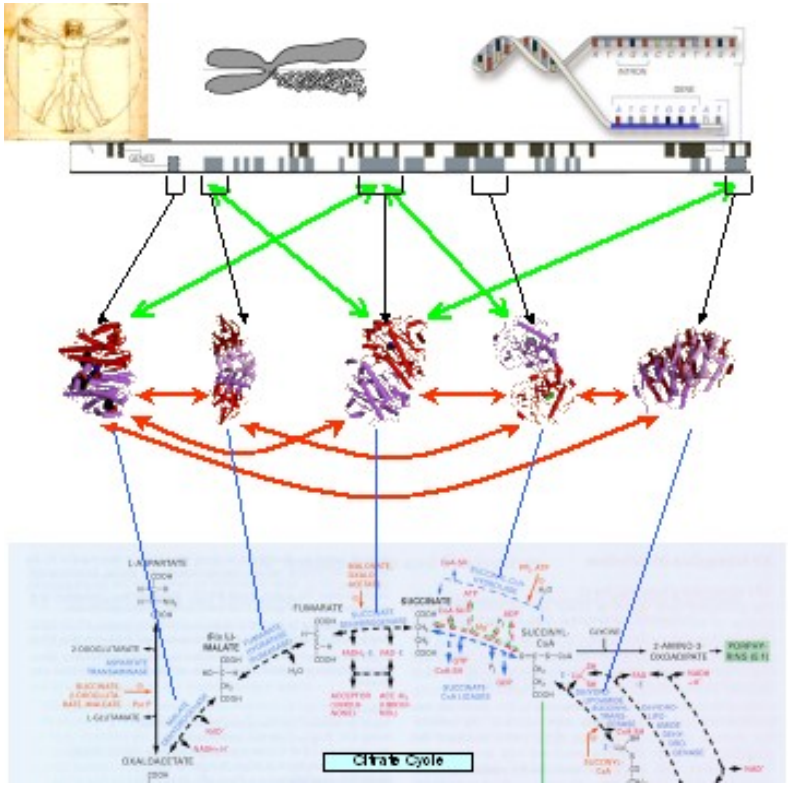

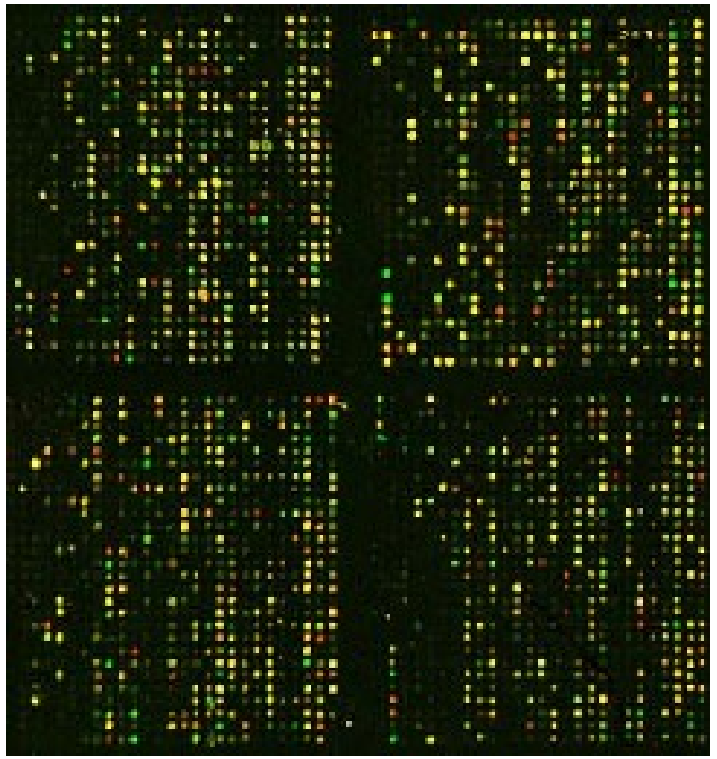

Networks in the cell appear at many levels. They include protein-protein interaction networks (red-lines), protein-gene intereactions (green-lines) and metabolic networks (bottom). They together form what is often called the "cellular network."

Metabolomics

- **Genomics and proteomics tell you what might happen, but metabolomics tells you what actually did happen.**

- Bill Lasley-
University of California, Davis

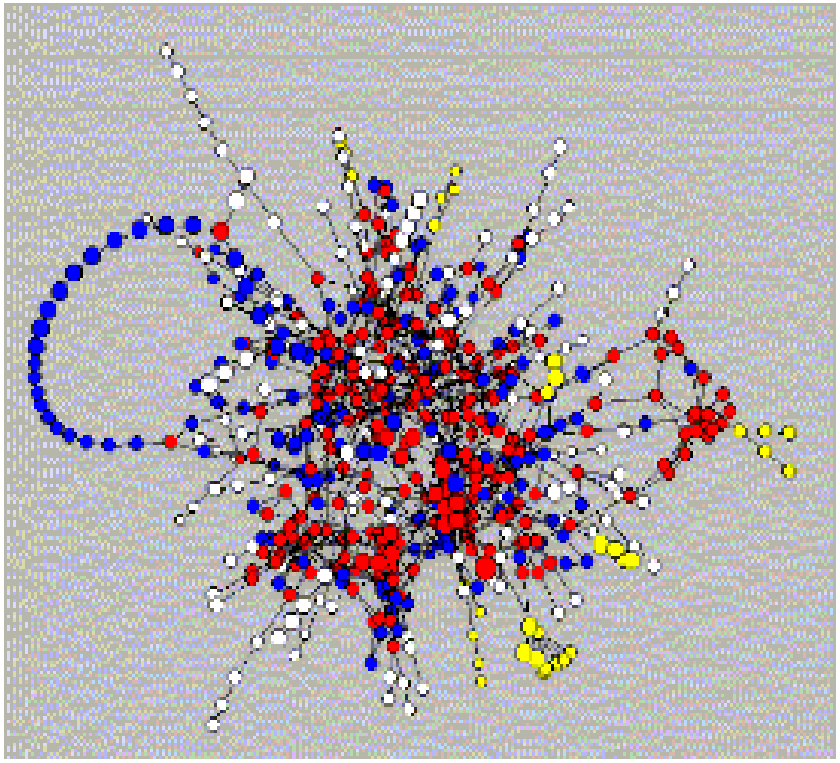

The topology of the metabolic network of the yeast cell

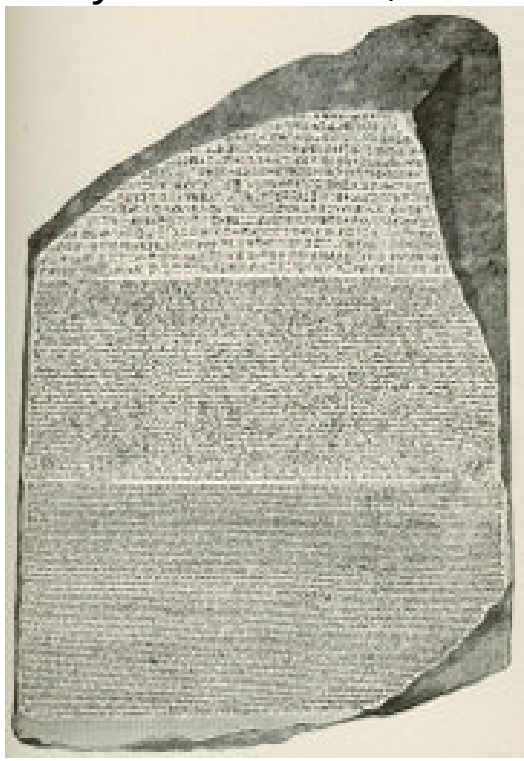

The Rosetta Stone

Metabolomics

Jens Nielsen
Professor, dr. techn., Ph.D.

- The fraction of open reading frames (ORFs) in a given genome directly involved in cellular metabolism is relatively low

TABLE 1. Overview of reactions, metabolites, and ORFs in reconstructed metabolic networks[a]

Organism	No. of reactions	No. of metabolites	No. of metabolic ORFs	Total no. of ORFs	% of ORFs involved in metabolism
H. pylori	444	340	268	1,638	16
H. influenzae	477	343	362	1,880	19
E. coli	720	436	695	4,485	15
S. cerevisiae	1,175	584	708	5,773	12[b]

[a] The reconstructed networks are described in references 6, 8, 17, and 18.
[b] The value is based on a recent gene count (3).

Guest commentary 2003 Journal of Bacteriology Vol.185,No.24

Metabolomics

- The reconstructed networks clearly illustrate how the different parts of the cellular metabolism are interconnected, particularly due to usage of common factors like ATP, ADP, NADH, and NADPH .it is not only these factors that ensure a tight connection among the different branches of the metabolic network.

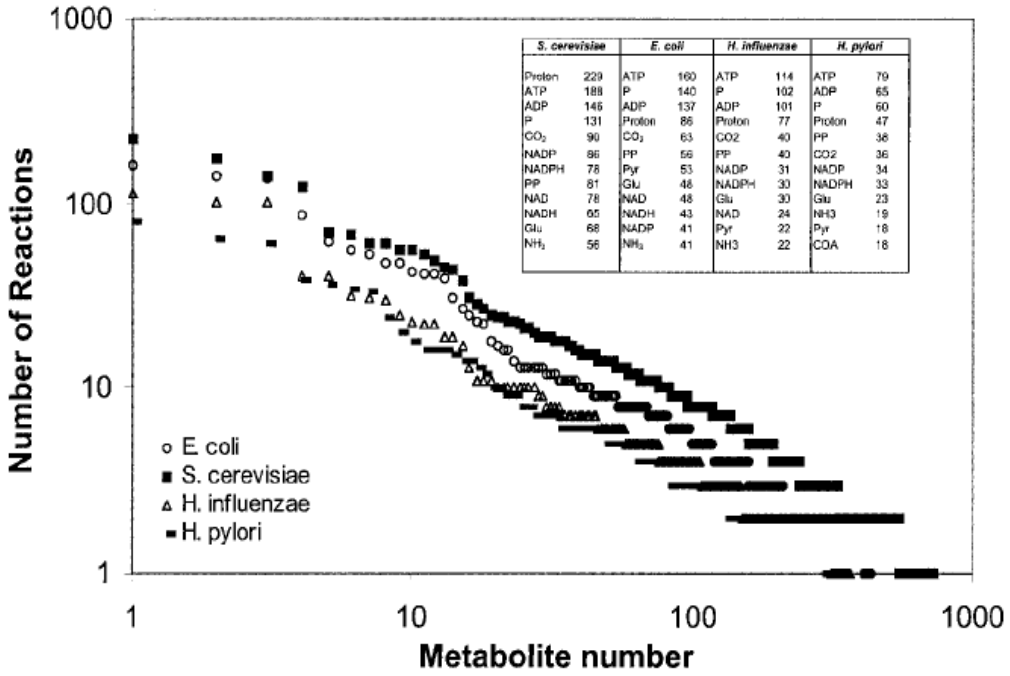

S. cerevisiae		E. coli		H. influenzae		H. pylori	
Proton	229	ATP	160	ATP	114	ATP	79
ATP	188	P	140	P	102	ADP	65
ADP	146	ADP	137	ADP	101	P	60
P	131	Proton	86	Proton	77	Proton	47
CO_2	90	CO_3	63	CO2	40	PP	36
NADP	86	PP	56	PP	40	CO2	36
NADPH	78	Pyr	53	NADP	31	NADP	34
PP	81	Glu	48	NADPH	30	NADPH	33
NAD	78	NAD	48	Glu	30	Glu	23
NADH	65	NADH	43	NAD	24	NH3	19
Glu	68	NADP	41	Pyr	22	Pyr	18
NH_3	56	NH_3	41	NH3	22	COA	18

Changes in fluxes in one part of the metabolism disseminate to many other parts of the metabolism, resulting in a global response

Guest commentary 2003 Journal of Bacteriology Vol.185,No.24

The Analyzing tools

- Not only need to accommodate the high diversity of biomolecules but also need to cover the vast dynamic range
- Extreme care and fast inactivation of all biochemical reactions during sampling vs. Proteome &. Transcriptome
- **Dynamic Range**: The range of concentrations, between detection limit and maximum amount of a substance to be quantified by one analytical technology
- Spectroscopy fingerprint at infrared (IR) , near infared (NIR), or UV , GC-MS, LC-ESI-MS, CE-MS, LC-NMR--------No single analytical platform for the complete metabolome

(Metabolome analysis , trends in biotechnology, vol.23 No.1 Jan 2005)

The Analyzing Tools

Table 1. Overview of the four general variants in the toolbox of metabolome analyses. Properties of fingerprinting, profiling, pool size and flux analysis are described for typical analyses

	Fingerprinting	Profiling	Pool size analysis	Flux analysis
Major field of application	Functional genomics, diagnostics	Functional genomics, molecular physiology	Biochemistry, biotechnology, molecular physiology	Biotechnology, modeling
Major result	Sample classification based on apparent metabolite pattern	Relative quantification of changes in metabolite pool size, identification and discovery of novel metabolites	Absolute quantification of metabolite pools	Quantification of metabolite flux
Sample composition	High complexity (minimal pre-purification)		Low complexity (partial or highly selective purification)	High complexity (minimal prepurification) possible
Sample throughput	High	High-medium	Low (might be extremely high when dedicated to a single metabolite)	Medium–low
Analytical technology	Nonhyphenated technologies possible	Hyphenated technologies required	Combination of hyphenated or nonhyphenated technologies (dependent on the means of prepurification)	
Metabolite coverage	Limited only by choice of metabolite extraction and analytical technology		Preconceived, that is, limited to a predefined set of targeted metabolites	
	Fingerprinting	**Profiling**	**Pool size analysis**	**Flux analysis**
Metabolite identification	Identification of metabolites not required	Identification of as many metabolites as possible	Unambiguous metabolite identification required	Unambiguous metabolite and mass isotopomer identification required
Metabolite concentrations	The concentration of the most abundant metabolite determines the highest possible sample load. The dynamic range of the instrument defines the detection limit of coanalyzed minor metabolites		Prepurification enables concentration of trace metabolites and thus adaptation to the sensitivity range of the analytical instrument. The dynamic range of instrumental analysis is thus nonlimiting.	
Required control experiments	Detector response is corrected for the initial amount of sample and total losses of material during sample preparation and handling	In addition, analysis of recovery, detection limits and linearity of detector response of all known metabolites	In addition, quantitative calibration of the detector response by dilution of a series of pure metabolites	In addition, tracer experiments with radioactive or stable isotope-labeled metabolites
Analytical trade-off	The precision of metabolite identification and quantification is sacrificed for optimised sample through-put.	Absolute quantification is substituted for relative quantification in exchange for full metabolite coverage and medium to high sample throughput	The number of analyzed metabolites is restricted in exchange for precise quantification	The number of analyzed metabolites is restricted in exchange for precise quantification of metabolite mass isotopomers

Quatitative metabolite profiling by mass isotopomer ratios

Box 1. Experimental set-up of mass isotopomer ratio profiling

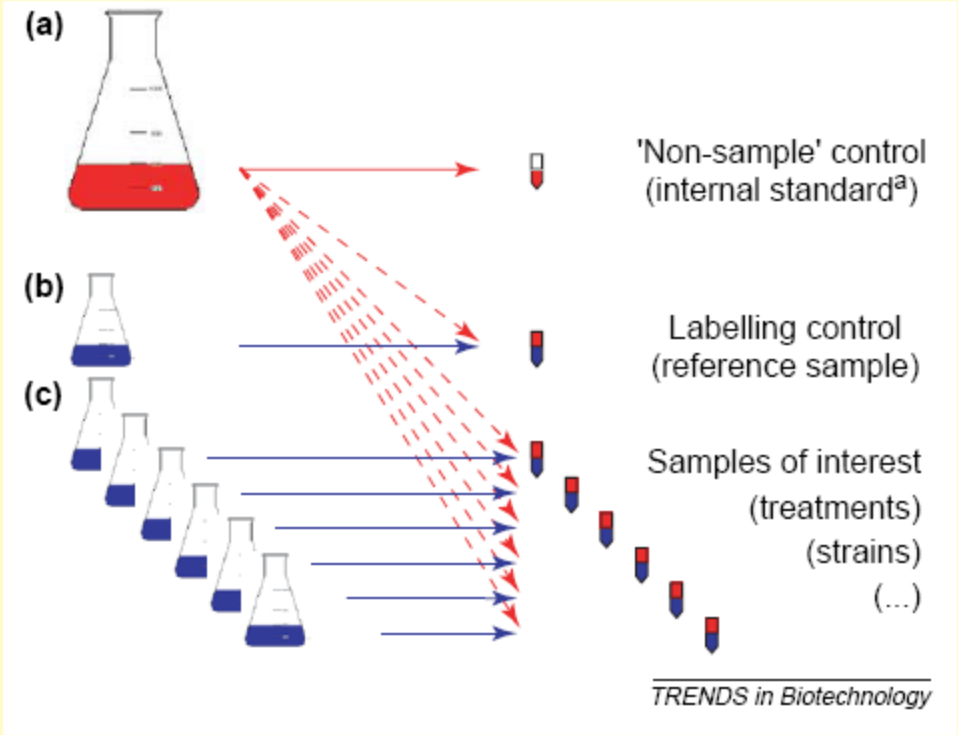

A: a yeast parent strain is grown on pure U-C13-glucose in synthetic defined media (red)

B: an identical culture is prepared with unlabeled glucose (blue)

C: experiments on different strains or treatments are performed with unlabeled carbon sources (blue). Equal amounts of culture A are combined with samples of B or C. Labeled samples serve as analytical internal standards and are typically monitored by “non-sample” controls. The labeling control B checks for inherent changes owing to C13-labeling.Relative changes in metabolite pool size are determined by mass isotopomer ratio, as exemplified in Box 3

Comparison of gas chromatography-mass spectrometry (GC-MS) spectra from separate 13C-labeled and 12C-metabolite preparations

Box 2. Head to tail comparison of gas chromatography–mass spectrometry (GC-MS) spectra from separate ^{13}C-labeled and ^{12}C-metabolite preparations

In Figure II mass spectra show the number of carbon atoms in all those mass fragments which originate from metabolites.

1: High labeling efficiency is essential because the chances of obtaining a fully labeled mass isotopomer decrease when atom numbers increase (see Glossary). Up to C_{28}, we found unambiguous mass isotopomer distribution in metabolites from yeast grown on pure U-^{13}C-glucose (99 atom %).

2: Incomplete labeling, although insufficient for the determination of high carbon numbers, still enables quantification by mass isotopomer ratios. For high molecular weight metabolites, *in vivo* labelling of less abundant elements, for example N, chemical tagging or analysis of low molecular weight constituents is advisable, such as are employed in proteome analysis [41,42].

3: Addition of unlabeled essential vitamins and auxotrophic supplements to microbial cultures causes respective products to be unlabeled. For example, we found NAD^+ to be fully labeled at the 15 carbon atoms which are ultimately synthesized from glucose. The residual six carbon atoms resulting from the nicotinic acid vitamin supplement were unlabeled.

[a]The GC-MS metabolite profiling requires chemical derivatization by N-methyl-N-(trimethylsilyl)-trifluoroacetamide (MSTFA). This reagent introduces a specific number of trimethylsilyl moieties (TMS) to each metabolite molecule, as is indicated in brackets.

[b]Mass fragments at 73 and 147 mass units are generated exclusively from TMS moieties.

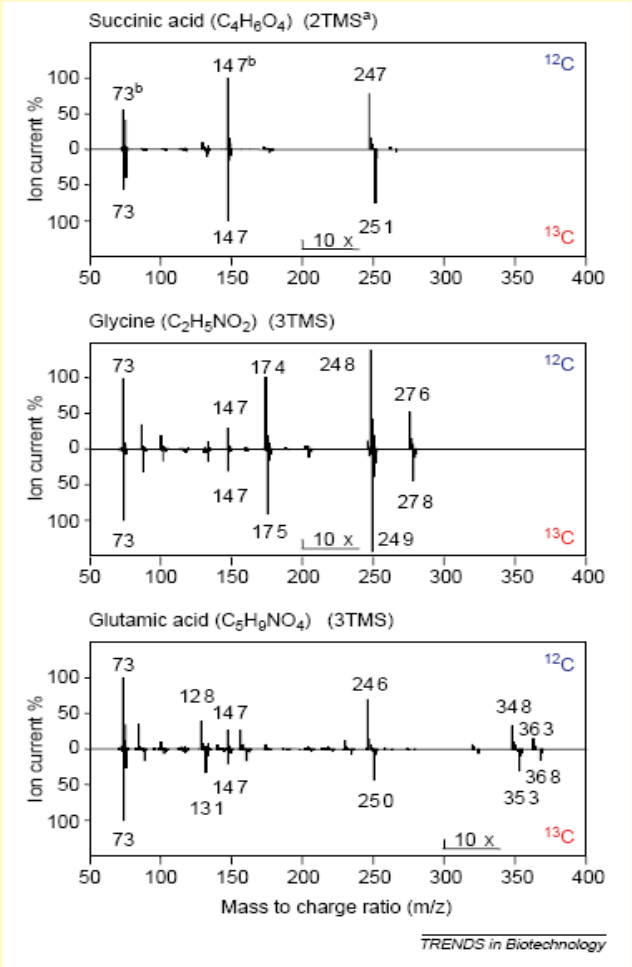

Figure II.

Quantification by gas chromatography- mass spectrometry mass isotopomer ratio profiling

Box 3. Quantification by gas chromatography–mass spectrometry mass isotopomer ratio profiling

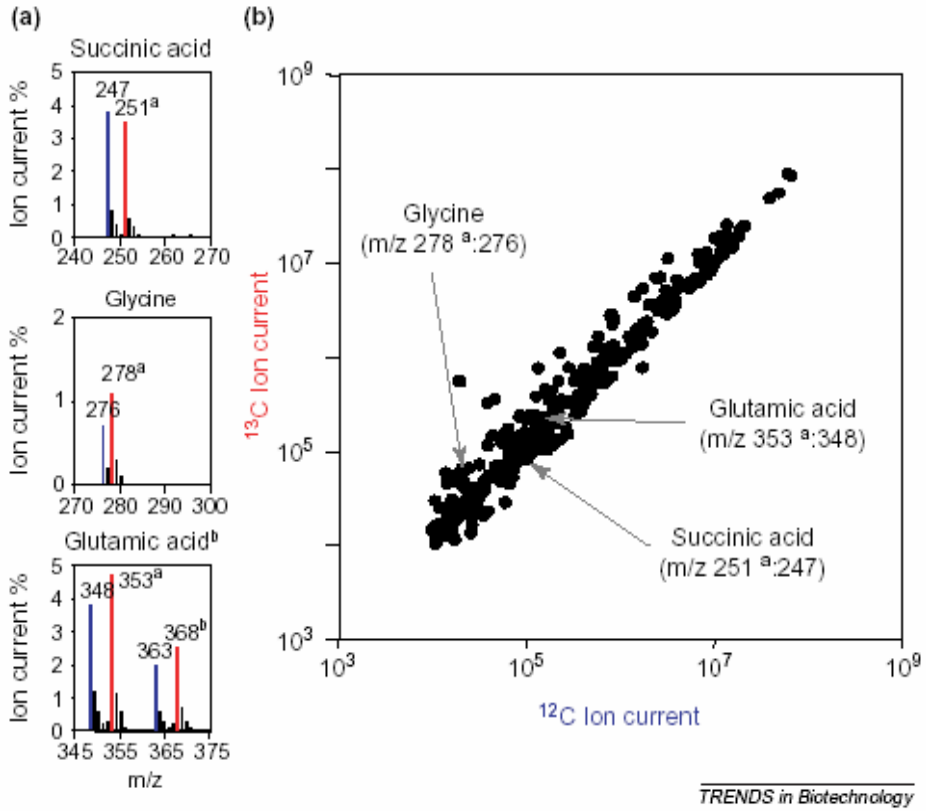

Figure II. **(a)** shows fragment pairs of labeled and unlabeled mass isotopomers representing the same metabolite. Ion currents reflect the relative changes in metabolite abundance. **(b)** Plot of labeled over unlabeled metabolite fragments from a mass isotopomer ratio profile, demonstrating that yeast cultures – in this case overnight batch cultures – exhibit small but perceptible changes in metabolite levels upon *in vivo* ^{13}C labeling (This plot represents the labeling control experiment shown in in Box 1).
[a]Mass fragments which represent the ^{13}C-labeled mass isotopomer, that is, the specific internal standard for this metabolite.
[b]Metabolites can be monitored by one or multiple mass isotopomer pairs for quantification and confirmation.
[c]Labeled mass isotopomers, especially those with fewer than three carbon atoms, are best corrected for natural stable mass isotopes.

Where for labeling analysis?

- Target 1----Cellular constituents formed during growth of the examined cells. Like amino acids from the cell protein, nucleotides from DNA, or monomers from glycogen
- Non-growing cells, eg. In production processes of primary or secondary metabolites
- Target 2---Secreted products
- This requires sufficient amounts of the products to be analyzed, no interference with medium components and case-specific development of analytical protocols for the analytes of interest

Labeling analysis of CO2

The use of membrane serving as a gas inlet for a mass spectrometer

The sample passes continuously along a microporous PTEE-membrane separating the liquid from the gaseous phase

Volatile substances (CO2) contained in the solution evaporate through the membrane pores in the vacuum system of the analyser

Membrane inlet mass spectrometry

Capillary inlet mass spectrometry

Membrane inlet system

Tae Hoon Yang et.al Computational biology and chemistry 29 (2005) 121-123

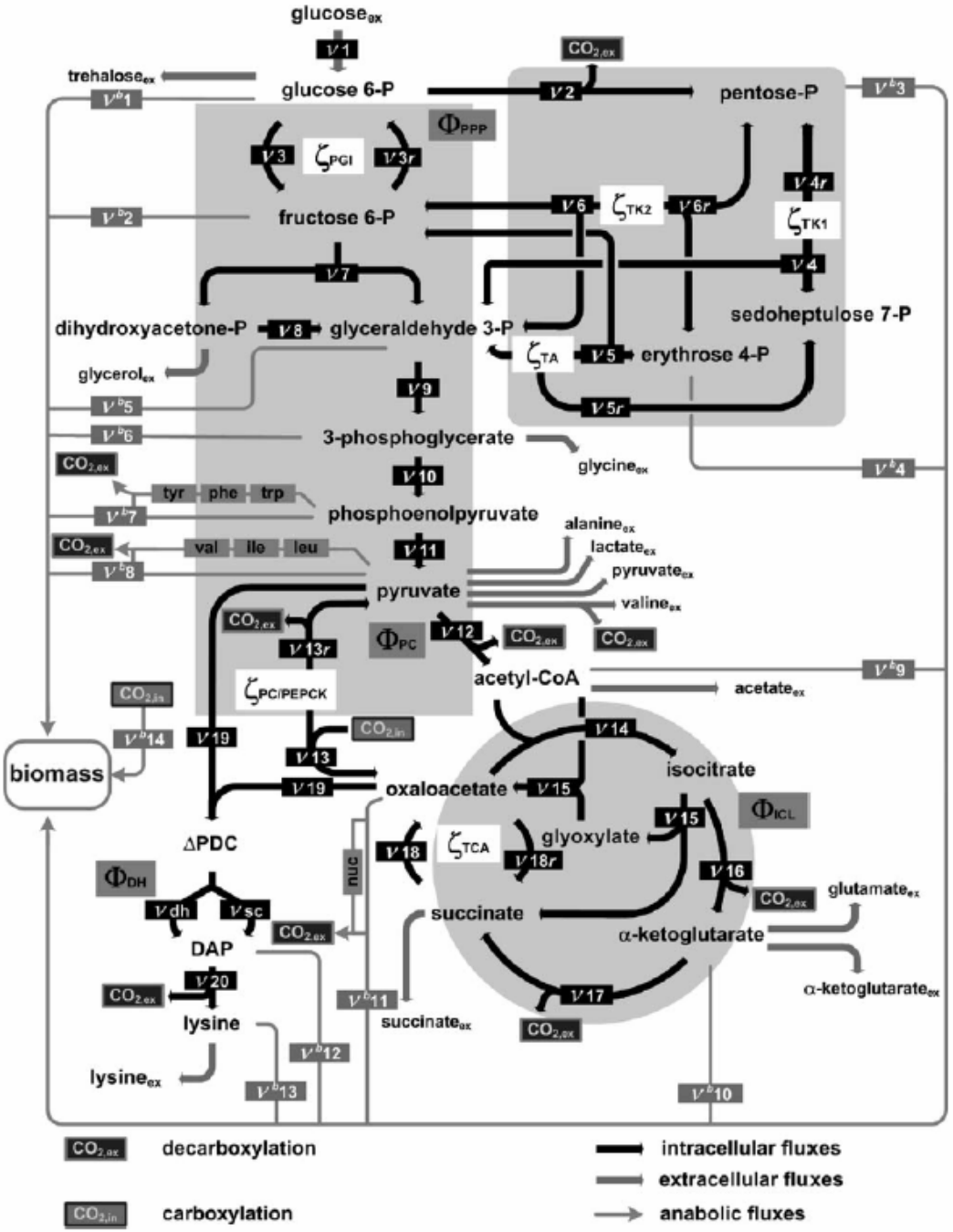

- Metabolic network model of *C. glutamicum*
- Definitions for the flux parameters (Φi, ζi) are given in Table 2. v, fluxes; vb, anabolic fluxes
- The subscript ‘ex’ indicates extracellular pools of substrates and products.

Tae Hoon Yang et al. Computational Biology and chemistry 29 2005 121-133

Modeling of respirometric C13 metabolic flux analysis

Table 1
Decarboxylation and carboxylation reactions in catabolic and anabolic pathways of *C. glutamicum* including corresponding precursor/product, enzyme, the atom mapping matrix (AMM) for the carbon atom transfer from the precursor to CO_2 and the stoichiometric consumption/production during biomass formation

Decarboxylation

Pathway	Precursor	Enzyme	AMM	Production[a] (μmol/g dcw)
v_2	Glucose 6-P	6-Phosphogluconate dehydrogenase	[1 0 0 0 0 0]	
v_{12}	Pyruvate	Pyruvate dehydrogenase complex	[1 0 0]	
v_{13r}	Oxaloacetate/malate	Phosphoenolpyruvate carboxykinase/malic enzyme, oxaloacetate decarboxylase	[0 0 0 1]	
v_{16}	Isocitrate	Isocitrate dehydrogenase	[0 0 0 0 0 1]	
v_{17}	α-Ketoglutarate	α-Ketoglutarate dehydrogenase	[1 0 0 0 0]	
v_{20}	*meso*-Diaminopimelate	*meso*-Diaminopimelate decarboxylase	[0 0 0 0 0 0 1]	
$Valine_{ex}$	Pyruvate	Acetohydroxy acid synthase	[1 0 0]	
v_7^b (Tyrosine)	Phosphoenolpyruvate	Prephenate dehydrogenase	[1 0 0]	81
v_7^b (Phenylalanine)	Phosphoenolpyruvate	Prephenate dehydrogenase	[1 0 0]	133
v_7^b (Tryptophan)	Phosphoenolpyruvate	Indoleglycerol phosphate synthase	[1 0 0]	54
v_8^b (Valine)	Pyruvate	Acetohydroxy acid synthase	[1 0 0]	284
v_8^b (Isoleucine)	Pyruvate	Acetohydroxy acid synthase	[1 0 0]	202
v_8^b (Leucine)	Pyruvate (2 mol)	Acetohydroxy acid synthase Isopropylmalate dehydrogenase	[1 0 0] [1 0 0]	440 440
v_{11}^b (Nucleotides)	Oxaloacetate	Orotidine monophosphate decarboxylase during pyrimidine nucleotide biosynthesis	[1 0 0 0]	310

Carboxylation

Pathway	Product	Enzyme	Consumption[a] (μmol/g dcw)
v_{13}	Oxaloacetate	Pyruvate carboxylase/phosphoenolpyruvate carboxylase	
v_{14}^b	Arginine	Carbamoyl-P-synthase	189
v_{14}^b	DNA, RNA	Phophoribosylaminoimidazole carboxylase during purine nucleotide, carbamoyl-P-synthase during pyrimidine nucleotide biosynthesis	730

Since CO_2 has only one carbon atom, the carbon atom transition involved in each pathway from a precursor with n carbons to CO_2 is represented by an AMM with $1 \times n$ dimension. The numbering of the reactions corresponds to the metabolic network used (Fig. 1).

[a] Amount of carbon dioxide produced or consumed for 1 g of biomass synthesis for *C. glutamicum* (Marx et al., 1996).

Tae Hoon Yang et al. Computational Biology and chemistry 29 2005 121-133

The Key Model Paraters

- Measurable extracellular fluxes v^{ext}
- Anabolic fluxes v^{b}
- Intracellular fluxes v^{var}

$$z_f = (\Phi_1, \Phi_2, \ldots | \zeta_1, \zeta_2, \ldots | v_1^{ext}, v_2^{ext}, \ldots | v_1^{b}, v_2^{b}, \ldots)^T:$$

$$v^{var} = N_v(z_f). \quad (1)$$

Here, $N_v = (n_{v,1}, n_{v,2}, \ldots, n_{v,m})^T$ is a system consisting of particular analytical expressions ($n_{v,i}$) for each flux. To exclude a physiologically meaningless range of the fluxes, $v < 0$, the range of the independent variables is set by $z_f = \{z_f \in \Re^k | \forall z_{f,i} \geq 0 \wedge \forall n_{v,i}(z_f) \geq 0\}$ with k being the dimension of z_f.

- Flux partitioning ratio Φi with respect to net flux distributions around the key branch points of metabolism
- Reaction reversibilities ζi with respect to the reversibilities of reactions of interest without varying their net fluxes

Tae Hoon Yang et al. Computational Biology and chemistry 29 2005 121-133

Definitions and literature values of key flulx parameters of the wild type C.glutamicum ATCC 12032 and the lysine-producing mutant C.glutamicum ATCC 21526.

Table 2

Definitions and literature values (Wittmann and Heinzle, 2002) of key flux parameters of the wild type *C. glutamicum* ATCC 13032 and the lysine-producing mutant *C. glutamicum* ATCC 21526, including flux partitioning ratios (Φ_i) and reversibilities (ζ_i)

Flux parameters	*C. glutamicum* ATCC 13032	*C. glutamicum* ATCC 21526
Flux partitioning ratio		
EMP and PP pathway: $\Phi_{PPP} = \nu_2/(\nu_2 + \nu_3 - \nu_{3r})$	0.52	0.61
Anaplerosis and TCA: $\Phi_{PC} = (\nu_{13} - \nu_{13r})/(\nu_{12} + \nu_{13} - \nu_{13r})$	0.18	0.28
Glyoxylate shunt and TCA: $\Phi_{ICL} = \nu_{15}/(\nu_{15} + \nu_{16})$	0	0
Succinylase and dehydrogenase pathway: $\Phi_{DH} = \nu_{dh}/(\nu_{dh} + \nu_{sc})$	0.23	0.11
Reversibility		
Glucosephosphate isomerase in EMP: $\zeta_{PGI} = \nu_{3r}/(\nu_3 - \nu_{3r})$	6.9	7.5
Pyruvate in EMP $\leftrightarrow$ oxaloacetate in TCA: $\zeta_{PC/PEPCK} = \nu_{13r}/(\nu_{13} - \nu_{13r})$	1.3	0.8
Transketolase 1 in PP pathway: $\zeta_{TK1} = \nu_{4r}/(\nu_4 - \nu_{4r})$	2.5	2.5
Transketolase 2 in PP pathway: $\zeta_{TK2} = \nu_{6r}/(\nu_6 - \nu_{6r})$	0.5	0.5
Transaldolase in PP pathway: $\zeta_{TA} = \nu_{5r}/(\nu_5 - \nu_{5r})$	1	1
Oxaloacetate $\leftrightarrow$ succinate in TCA: $\zeta_{TCA} = \nu_{18r}/(\nu_{18} - \nu_{18r})$	25	8.1

The reaction numbering corresponds to the metabolic network in Fig. 1.

Tae Hoon Yang et al. Computational Biology and chemistry 29 2005 121-133

Isotopomer network

- Each compound with *n* carbons exhibits 2^n possible labeling states, so these models are inherently complex
- IDV --- isotopomer distribution vectors
- IMM --- isotopomer mapping matrices
- AMM --- atom mapping matrices

Atom Mapping Matrices

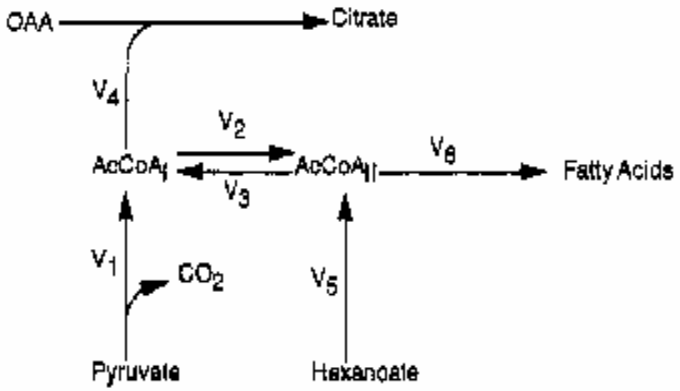

Figure 1. Simple metabolic network for modeling AcCoA metabolism. V_1–V_6 represent fluxes (typical units: millimoles/cell/hour). Pyruvate and hexanoate are potentially labeled substates (based on network analyzed by Blum and Stein (1982)).

$$A + B \xrightarrow{E} C + D$$

$[A>C]_E$ describes transfer of carbon from A to C

$[A>D]_E$ describes transfer of carbon from A to D

$[B>C]_E$ describes transfer of carbon from B to C

$[B>D]_E$ describes transfer of carbon from B to D

$$[A>C]_E A + [B>C]_E B = C$$

$$[A>D]_E A + [B>D]_E B = D$$

$$\mathbf{Pyr} = \begin{bmatrix} \mathrm{Pyr}(1) \\ \mathrm{Pyr}(2) \\ \mathrm{Pyr}(3) \end{bmatrix} \quad \mathbf{AcCoA_I} = \begin{bmatrix} \mathrm{AcCoA_I}(1) \\ \mathrm{AcCoA_I}(2) \end{bmatrix}$$

$$\mathbf{Hex} = \begin{bmatrix} \mathrm{Hex}(1) \\ \mathrm{Hex}(2) \\ \mathrm{Hex}(3) \\ \mathrm{Hex}(4) \\ \mathrm{Hex}(5) \\ \mathrm{Hex}(6) \end{bmatrix} \quad \mathbf{AcCoA_{II}} = \begin{bmatrix} \mathrm{AcCoA_{II}}(1) \\ \mathrm{AcCoA_{II}}(2) \end{bmatrix}$$

Zupke,C.& Stephanopoulous Biotechnol. Prog.1994,10,489-498

Atom Mapping Matrices

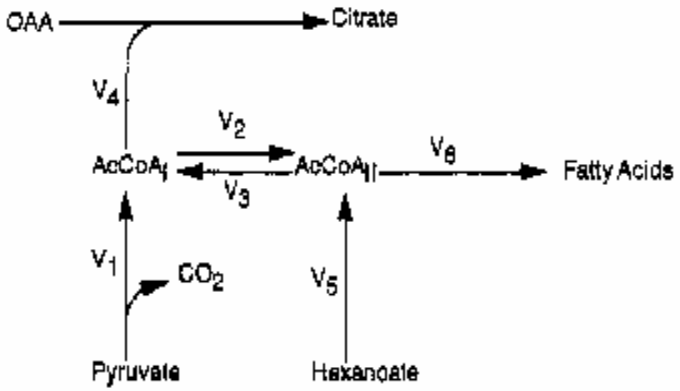

Figure 1. Simple metabolic network for modeling AcCoA metabolism. V_1–V_6 represent fluxes (typical units: millimoles/cell/hour). Pyruvate and hexanoate are potentially labeled substates (based on network analyzed by Blum and Stein (1982)).

The dimensions of the mapping matrices are determined by the number of carbons in the reactant and product. The number of columns equals the number of atoms in the reactant, while the number of rows equals the number of carbons in the product. The element in the ith row and the jth column of the mapping matrix specifies the amount of the ith carbon of the product that is derived from the jth carbon of the reactant. Typically, there is a definite and unique mapping of reactant carbons to product carbons, so that the elements of the mapping matrix are usually 0 or 1. However, fractional elements are possible.

$$[\mathbf{Pyr}>\mathbf{AcCoA_I}]_{\mathbf{PD}} = \begin{bmatrix} 0 & 1 & 0 \\ 0 & 0 & 1 \end{bmatrix}$$

$$[\mathbf{Pyr}>\mathbf{AcCoA_I}]_{\mathbf{PD}}\mathbf{Pyr} = \begin{bmatrix} 0 & 1 & 0 \\ 0 & 0 & 1 \end{bmatrix}\begin{bmatrix} \mathrm{Pyr}(1) \\ \mathrm{Pyr}(2) \\ \mathrm{Pyr}(3) \end{bmatrix} =$$

$$\begin{bmatrix} \mathrm{Pyr}(2) \\ \mathrm{Pyr}(3) \end{bmatrix} = \begin{bmatrix} \mathrm{AcCoA_I}(1) \\ \mathrm{AcCoA_I}(2) \end{bmatrix} = \mathbf{AcCoA_I}$$

$$[\mathbf{AcCoA_I}>\mathbf{AcCoA_{II}}]_{\mathbf{transI}} =$$

$$[\mathbf{AcCoA_{II}}>\mathbf{AcCoA_I}]_{\mathbf{transII}} = \begin{bmatrix} 1 & 0 \\ 0 & 1 \end{bmatrix}$$

$$[\mathbf{Hex}>\mathbf{AcCoA_{II}}]\beta_{\mathbf{ox}} = \begin{bmatrix} \frac{1}{3} & 0 & \frac{1}{3} & 0 & \frac{1}{3} & 0 \\ 0 & \frac{1}{3} & 0 & \frac{1}{3} & 0 & \frac{1}{3} \end{bmatrix}$$

Zupke,C.& Stephanopoulous Biotechnol. Prog.1994,10,489-498

Atom Mapping Matrices

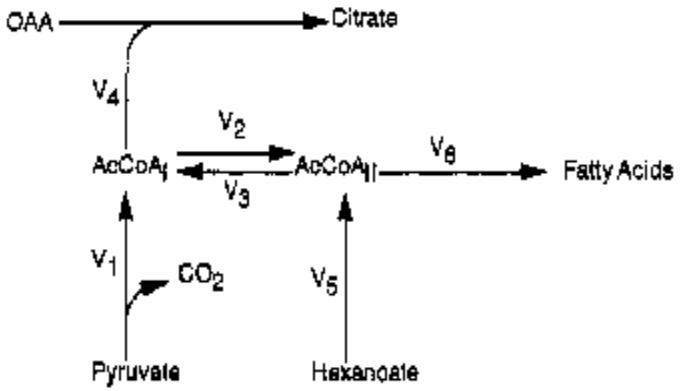

Figure 1. Simple metabolic network for modeling AcCoA metabolism. V_1–V_6 represent fluxes (typical units: millimoles/cell/hour). Pyruvate and hexanoate are potentially labeled substates (based on network analyzed by Blum and Stein (1982)).

$$\text{flux into } \mathbf{AcCoA_I} = V_1[\mathbf{Pyr} > \mathbf{AcCoA_I}]_{\mathbf{PD}}\mathbf{Pyr} + V_3[\mathbf{AcCoA_{II}} > \mathbf{AcCoA_I}]_{\mathbf{trans\,II}}\mathbf{AcCoA_{II}}$$

The flux of label out of $AcCoA_I$ is

$$\text{flux out of } \mathbf{AcCoA_I} = (V_2 + V_4)\mathbf{AcCoA_I}$$

Equating eqs 19 and 20 gives the steady state isotope balance for $AcCoA_I$:

$$(V_2 + V_4)\mathbf{AcCoA_I} = V_1[\mathbf{Pyr} > \mathbf{AcCoA_I}]_{\mathbf{PD}}\mathbf{Pyr} + V_2[\mathbf{AcCoA_{II}} > \mathbf{AcCoA_I}]_{\mathbf{trans\,II}}\mathbf{AcCoA_{II}}$$

Similarly, the steady state isotope balance for $AcCoA_{II}$ is

$$(V_3 + V_6)\mathbf{AcCoA_{II}} = V_2[\mathbf{AcCoA_I} > \mathbf{AcCoA_{II}}]_{\mathbf{trans\,I}}\mathbf{AcCoA_I} + V_5[\mathbf{Hex} > \mathbf{AcCoA_I}]_{\beta\mathbf{ox}}\mathbf{Hex}$$

Decouple the generation of the steady state quations from the details of the transfer of carbon atoms from reactants to products

Zupke,C.& Stephanopoulous Biotechnol. Prog.1994,10,489-498

C13 vs C14
(eg. Acetate molecule)

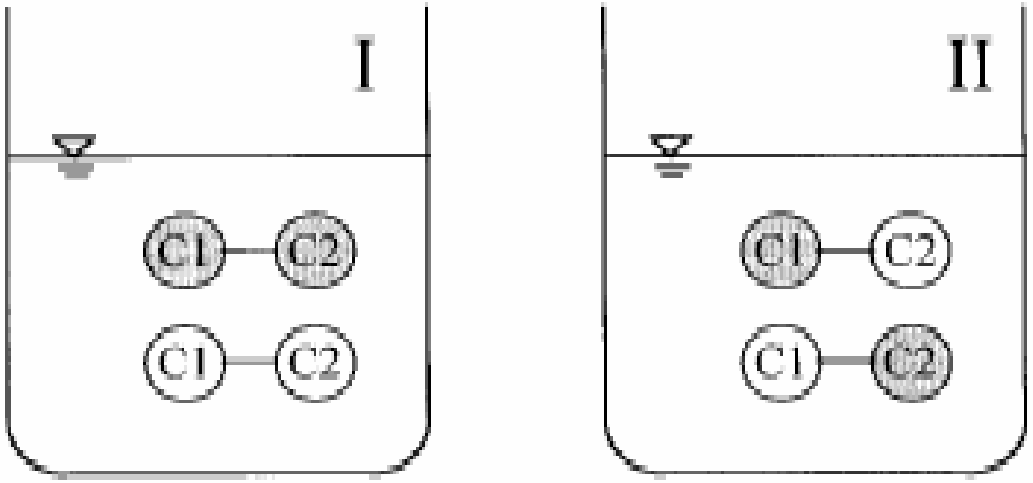

Figure 1. Two different isotopomer mixtures of a two carbon atom molecule. The shaded carbon atoms are labeled with either ^{13}C or ^{14}C.

Schmidt., K, Carsen.M, Nielsen.,J.Villadsen. Biotechnol.Bioeng 55:831-840,1997

Isotopomer distribution vectors

The IDV of glucose has $2^6 = 64$ elements. The first element of this column vector is indexed 0, i.e., specified as $\mathbf{I}_{\mathbf{glc}}(0)$. The zeroth element of the glucose IDV will contain a number between 0 and 1, representing the fraction of glucose molecules, showing the labeling pattern 000000_{bin} (unlabeled). The element at index 1 contains the mole fraction of glucose molecules labeled according to the binary number 000001_{bin}, meaning a single ^{13}C isotope in the sixth position in the glucose molecule. The mole fraction of [1-^{13}C]glucose is found at index 32 of the vector, because 32 is the decimal representation of the binary number (and labeling pattern) 100000_{bin}. By simple conversion of binary to decimal numbers, labeling patterns can easily be found for given index numbers and vice versa. The complete glucose IDV is given as

$$\mathbf{I}_{\text{glc}} = \begin{pmatrix} \mathbf{I}_{\text{glc}}(0) \\ \mathbf{I}_{\text{glc}}(1) \\ \mathbf{I}_{\text{glc}}(2) \\ \mathbf{I}_{\text{glc}}(3) \\ \cdots \\ \mathbf{I}_{\text{glc}}(63) \end{pmatrix} = \begin{pmatrix} \mathbf{I}_{\text{glc}}(000000_{\text{bin}}) \\ \mathbf{I}_{\text{glc}}(000001_{\text{bin}}) \\ \mathbf{I}_{\text{glc}}(000010_{\text{bin}}) \\ \mathbf{I}_{\text{glc}}(000011_{\text{bin}}) \\ \cdots \\ \mathbf{I}_{\text{glc}}(111111_{\text{bin}}) \end{pmatrix},$$

$$\text{with} \quad \sum_{i=0}^{63} \mathbf{I}_{\text{glc}}(i) = 1, \qquad (1)$$

where $\mathbf{I}_{\mathbf{glc}}(i)$ is the vector element at index i of the glucose IDV.

Isotopomer mapping matrices

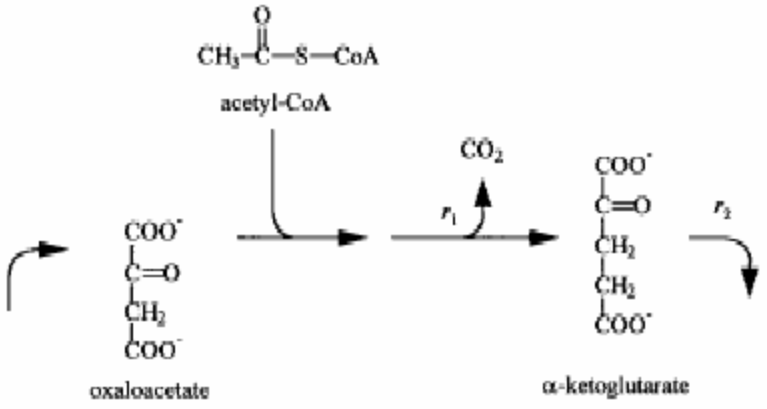

Figure 2. Entry of acetyl-CoA into the TCA cycle. r_1 is the molar rate of production and r_2 is the molar rate of consumption of α-ketoglutarate.

- The number of rows in IMM equals the number of vector elements in the product IDV. The number of columns of an IMM equals the number of vector elements of the reactant IDV.
- In the following, IMM names will be specified by subscripts containing two acronyms

Isotopomer mapping matrices

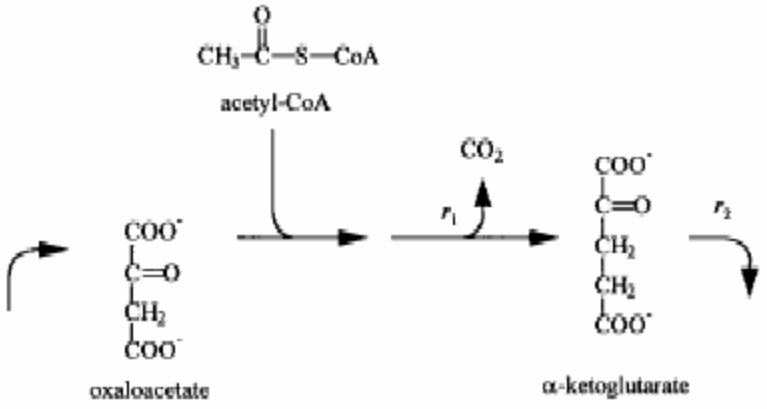

Figure 2. Entry of acetyl-CoA into the TCA cycle. r_1 is the molar rate of production and r_2 is the molar rate of consumption of α-ketoglutarate.

- The number of rows in IMM equals the number of vector elements in the product IDV. The number of columns of an IMM equals the number of vector elements of the reactant IDV.
- In the following, IMM names will be specified by subscripts containing two acronyms

Isotopomer network

- The distribution of the C13 label within the metabolic network can be computed by solving a system of stationary isotopomer balance equations

$$F_x(x, v) = 0.$$

Here, $F_x = (f_{x,1}, f_{x,2}, \ldots, f_{x,n})^T$ is an equation system containing n isotopomer balances ($f_{x,i}$) and x is the set of unknown isotopomer distribution vectors (IDV), $x = (x_1, x_2, \ldots, x_n)^T$. Each x given above is constrained such that $x_i = \{x_i \in \Re^{2^{n_c}} | \sum_{k=1}^{2^{n_c}} x_i(k) = 1 \wedge \forall k : 0 \leq x_i(k) \leq 1\}$, where n_c denotes the number of carbon atoms in the skeleton of a metabolite. A numerically stable and fast method for solving Eq. and thus calculating the isotopomer distributions for a given set of fluxes is described in Yang et al. (2004a).

Tae Hoon Yang et al. Computational Biology and chemistry 29 2005 121-133

Respirometric network

$$\sum_{i=1}^{p}(v_{CO_2,\text{in},i}s_i x^{\circ}_{CO_2,i}) - x_{CO_2}\sum_{j=1}^{q}(v_{CO_2,\text{out},j}s_j) = 0,$$

where $x^{\circ}_{CO_2}$ denotes the incoming IDV into the CO_2 pool, x_{CO_2} the IDV of CO_2, and s the stoichiometric coefficient of each reaction. Along with anabolic fluxes towards amino acids and macromolecules, carbon dioxide fluxes participating in those reactions can be directly calculated from the strain-specific data of precursor and carbon dioxide requirements (Table 1) (Neidhardt et al., 1990; Marx et al., 1996; de Graaf, 2000).

Tae Hoon Yang et al. Computational Biology and chemistry 29 2005 121-133

Experiment design

- Single output sensitivity
  [m+1] mass isotopomer fraction of CO2 ($^{m+1}fco_2$) towards change
  Of different key flux parameters in the central metabolism, i.e. partial
  Derivatives of $^{m+1}fco_2$
- D- optimality criterion

$$D(x^{\text{inp}}, y^{\text{ext}}_{\text{sim},M}; z_{\text{f}}) = \frac{1}{\det \text{Fish}(x^{\text{inp}}, y^{\text{ext}}_{\text{sim},M}; z_{\text{f}})},$$

where N_{f} is the number of independent variables considered. The larger the relative information index resulting from an experimental design, the more information can be predicted with respect to the input labeling pattern used for the reference experiment.

$$\bar{I} = \left(\frac{D_{\text{reference}}}{D_{\text{new design}}}\right)^{1/2N_{\text{f}}},$$

Tae Hoon Yang et al. Computational Biology and chemistry 29 2005 121-133

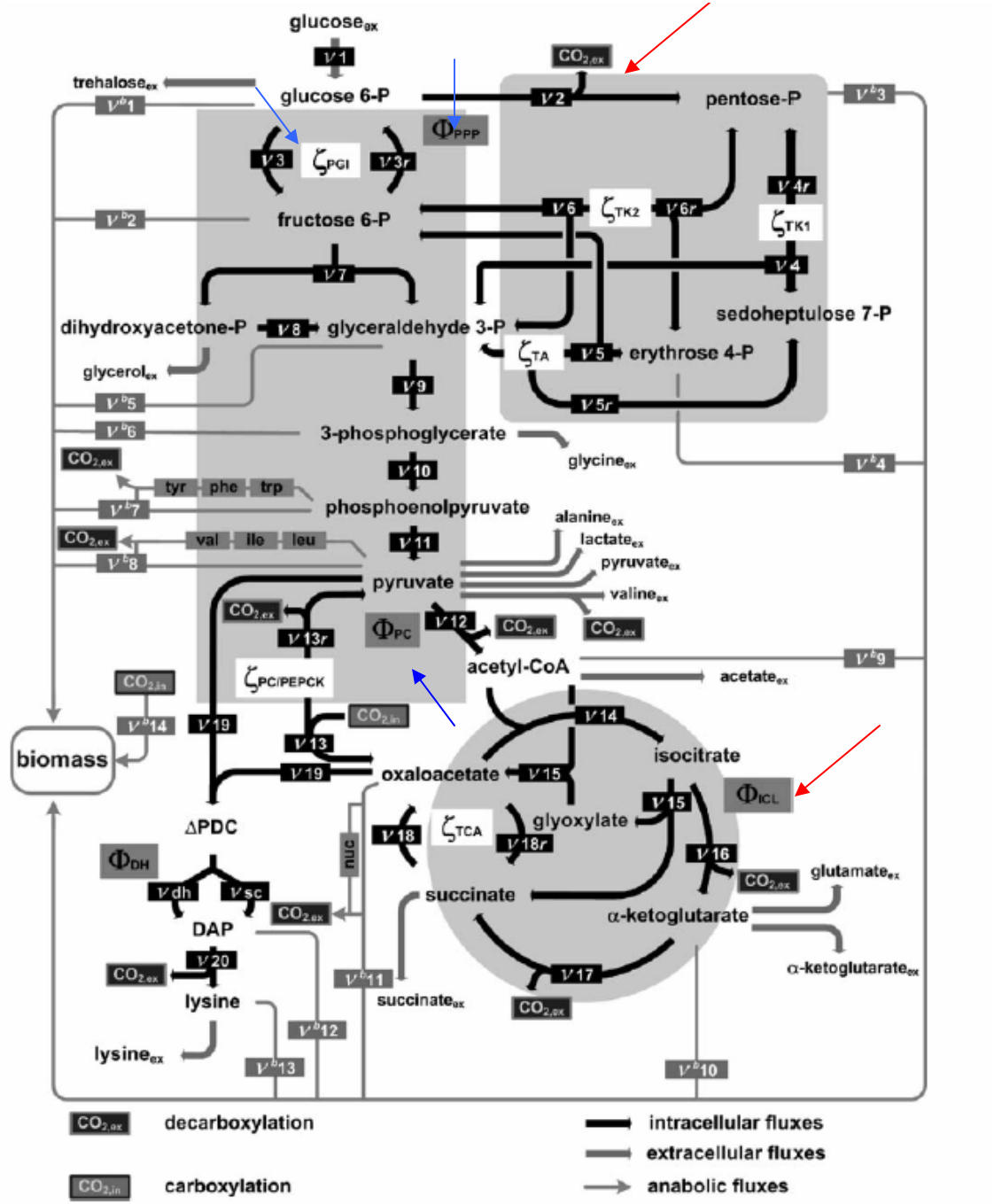

Tae Hoon Yang et al. Computational Biology and chemistry 29 2005 121-133

Primary identification of sensitive flux parameters by means of CO2 mass isotopomer analysis in the wild type C.glutamicum ATCC 13032(A-1,2,3), and the lysine-producing mutant C.glutamicum ATCC 21526 (B-1,2,3)

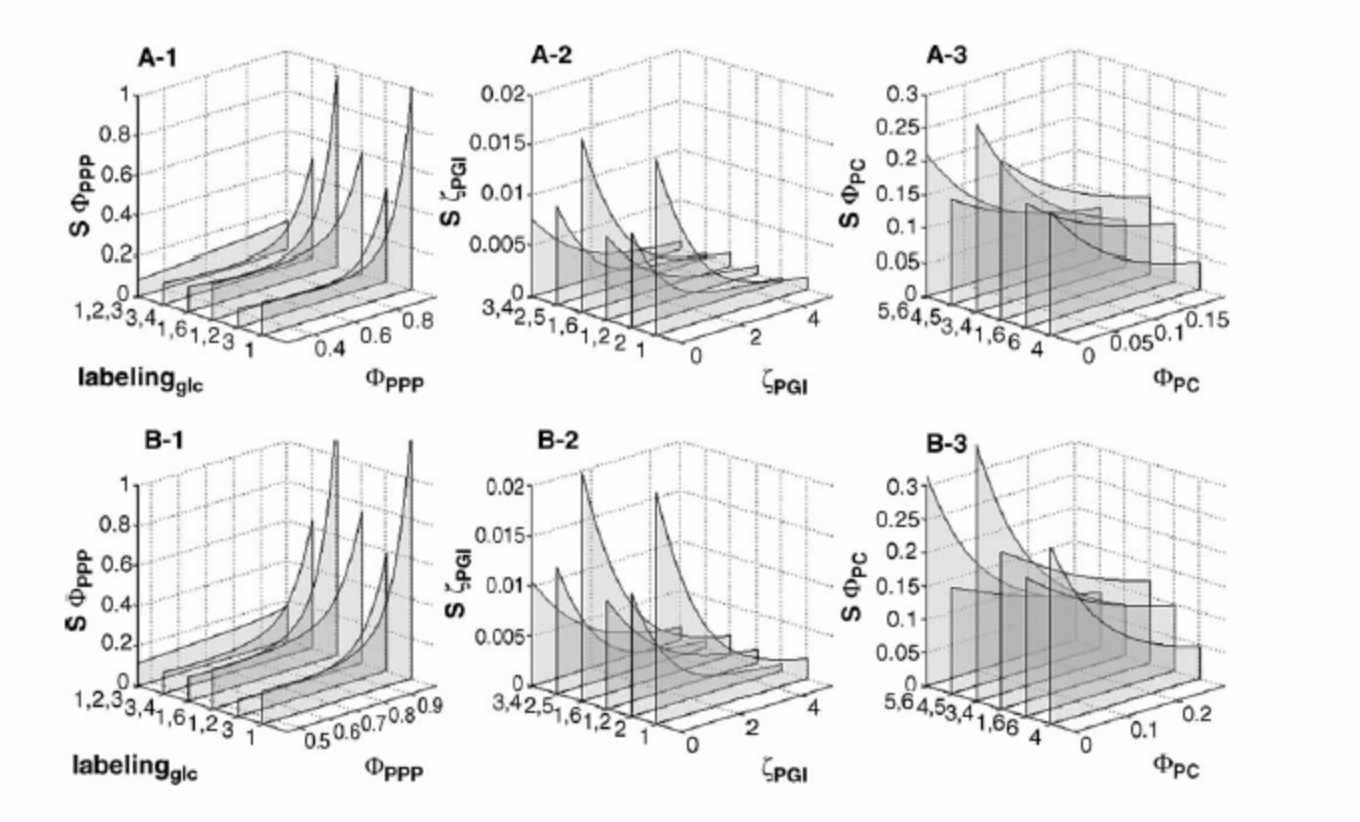

Tae Hoon Yang et al. Computational Biology and chemistry 29 2005 121-133

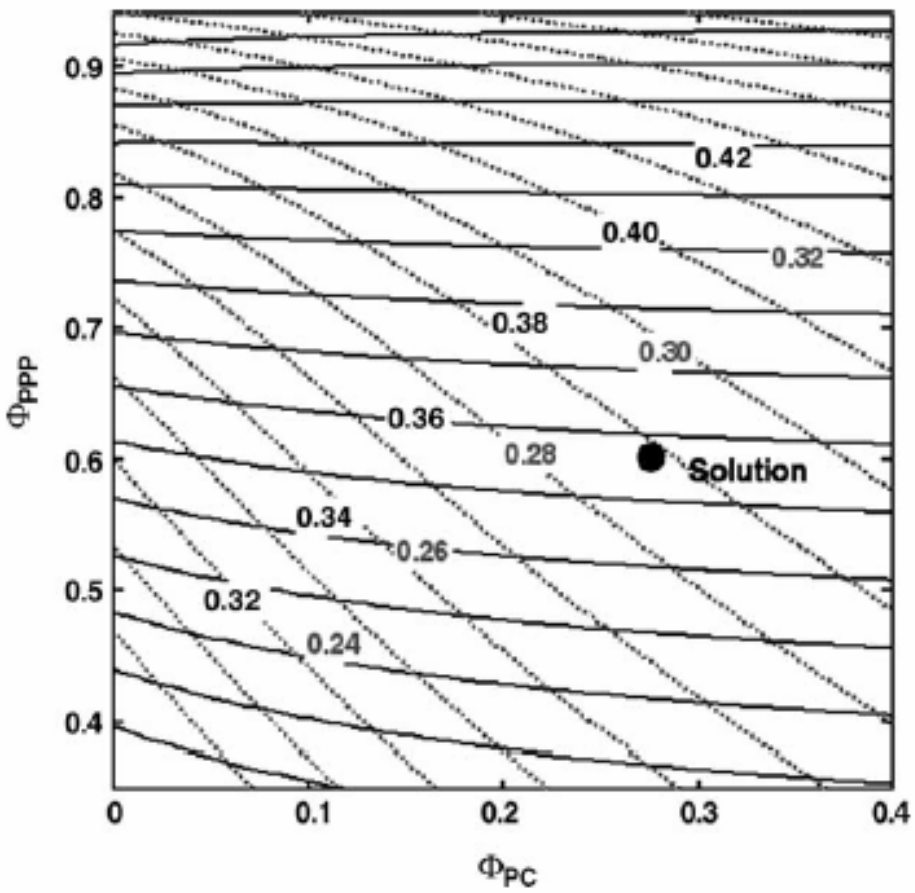

Fig. 3. Superimposed contour plots of $^{m+1}f_{CO_2}$ for simultaneous quantification of two flux parameters by use of two different input substrates: values of $^{m+1}f_{CO_2}$ resulting from [1,2-$^{13}C_2$] glucose (solid line, black) and [1,6-$^{13}C_2$] glucose (dotted line, gray) in the space of Φ_{PPP} and Φ_{PC} of the lysine-producing mutant *C. glutamicum* ATCC 21526. The real solution (●) is located at ($\Phi_{PPP} = 0.28$, $\Phi_{PC} = 0.61$) for the strain.

Tae Hoon Yang et al. Computational Biology and chemistry 29 2005 121-133

Optimal experimental design and relative information

$$z_f = T_{\rightarrow z_f}(\Phi_{PPP}, \Phi_{PC} | v_1^{ext}, v_2^{ext}, \ldots | Y_{X/S})^T.$$

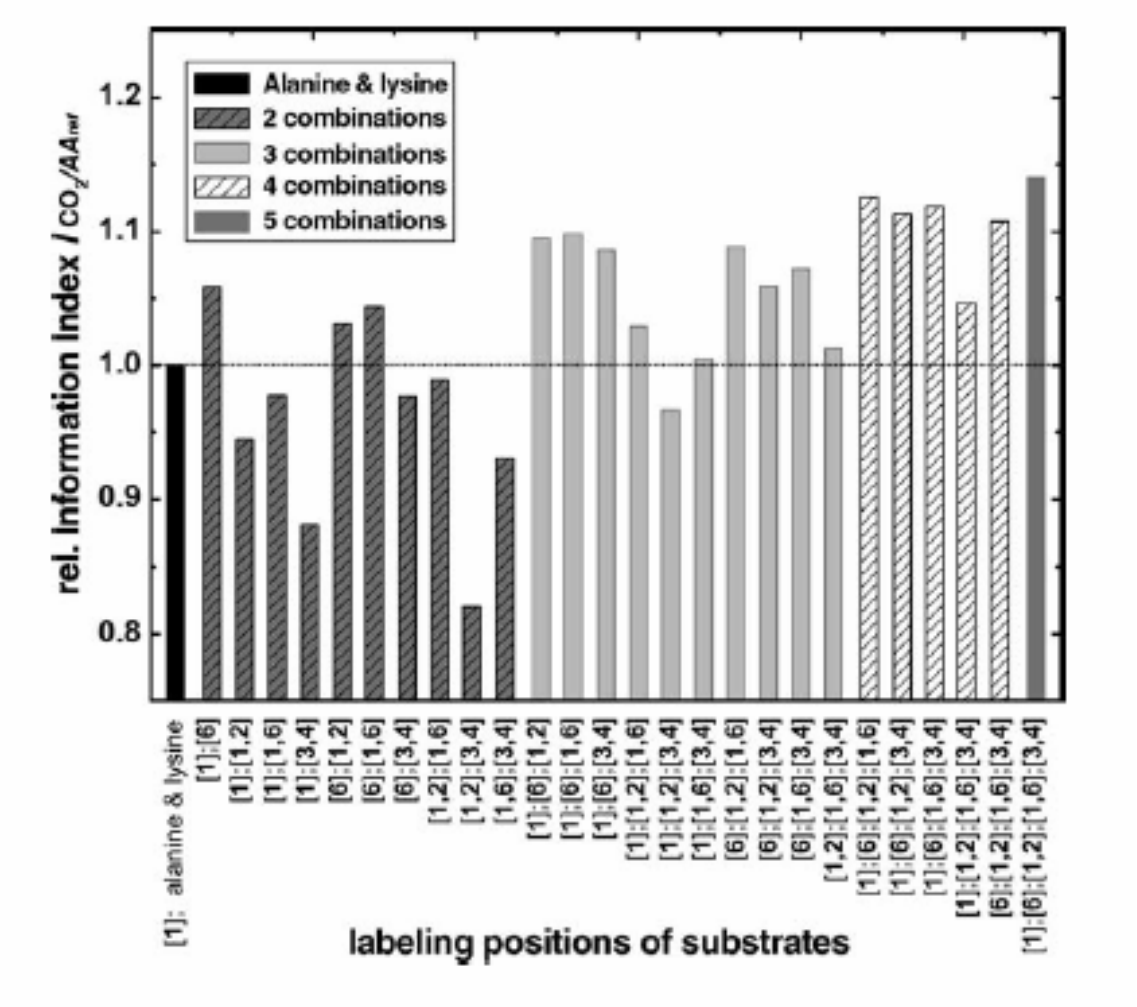

Optimal experimental design and relative information

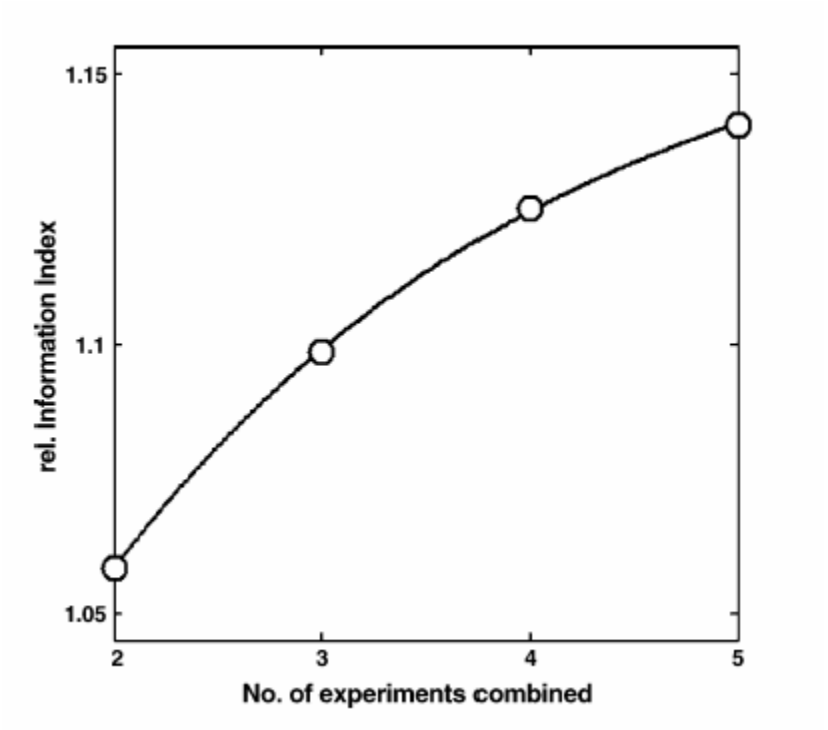

Tae Hoon Yang et al. Computational Biology and chemistry 29 2005 121-133

Optimal experimental design and relative information

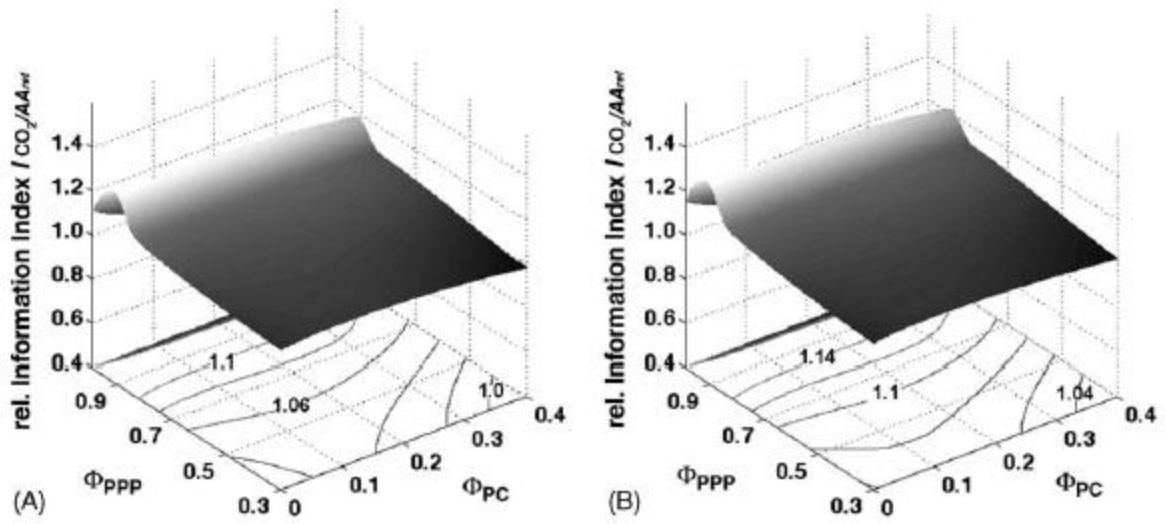

Relative information index ($I_{CO_2/AA_{ref}}$) in the space of Φ_{PPP} and Φ_{PC} predicted for the combined multiple tracer experiments [1-^{13}C] and [6-^{13}C] (A) and [1-^{13}C], [6-^{13}C] and [1,2-$^{13}C_2$] (B) for *C. glutamicum* ATCC 21526.

Tae Hoon Yang et al. Computational Biology and chemistry 29 2005 121-133

Summarize

- The respirometric approach complements existing methods for metabolic flux analysis. It is especially attractive for studies of non-growing cells. et.al.
- The accurate acquistion of production rates for single mass isotopomers of CO2 can be done by membrane inlet MS within a few minutes
- Applying miniaturized membrane probes, it seems even possible to apply this type of measurement to local determination of fluxes in tissues, sediments or immobilized cell systems.

Question?